





Cite this: DOI: 10.1039/c7dt00727b

A family of rhodium and iridium complexes with semirigid benzylsilyl phosphines: from bidentate to tetradentate coordination modes†

María Vicky Corona-González,^a Julio Zamora-Moreno,^a Cynthia A. Cuevas-Chávez,^{a,b,c} Ernesto Rufino-Felipe,^a Emmanuelle Mothes-Martin,^{b,c} Yannick Coppel,^{b,c} Miguel A. Muñoz-Hernández,^a Laure Vendier,^{b,c} Marcos Flores-Alamo,^d Mary Grellier,^{b,c} Sylviane Sabo-Etienne *^{b,c} and Virginia Montiel-Palma *^a

The synthesis of a new trisbenzylsilane phosphine P(*o*-C₆H₄CH₂)SiMe₂H)₃ (**1**) is shown to proceed with high yields from P(*o*-tolyl)₃. Compound **1** coordinates to the Rh and Ir dimers [MCl(COD)]₂ (M = Rh, Ir) in a tetradentate or tridentate fashion, depending on the strict exclusion of water. The dimeric compounds [ClM(SiMe₂CH₂-*o*-C₆H₄)₂P(*o*-C₆H₄-CH₂SiMe₂H)]₂, **2Rh** and **2Ir**, feature a tetradentate coordination of the starting ligand with P and two Si atoms as well as a non-classical agostic Si–H group. The presence of adventitious water in the solvents leads to the formation of two new complexes [(μ²-Cl)₂M₂(SiMe₂CH₂-*o*-C₆H₄)₂P(*o*-C₆H₄-CH₂SiMe₂OSiMe₂CH₂-*o*-C₆H₄-)P(SiMe₂CH₂-*o*-C₆H₄)₂], **3Rh** and **3Ir**, which feature a siloxane bridge through Si–H bond breaking in **2**. Reaction of [RhCl(COD)]₂ with the bisbenzylsilane phosphine PhP(*o*-C₆H₄CH₂)SiMe₂H)₂ leads to the formation of compound **4Rh** which features also a dimeric structure with the SiPSi ligand coordinated through the two silicon atoms, one of which occupies the apical position of a square-pyramidal geometry in the solid state, while the second is disposed equatorially *trans* to π-donor Cl. Finally, bidentate coordination of a PSi ligand is achieved by reaction of [RhCl(COD)]₂ with Ph₂P(*o*-C₆H₄CH₂)SiMe₂H which leads to the monometallic species [RhCl(SiMe₂CH₂-*o*-C₆H₄-PPh₂)₂], **5Rh**, incorporating two chelating PSi ligands and maintaining a Cl ligand.

Received 27th February 2017,
Accepted 31st March 2017

DOI: 10.1039/c7dt00727b

rsc.li/dalton

Introduction

Even the most superficial glance at the inorganic chemistry literature evidences an outburst in the number of studies related to silicon-substituted pincer,^{1–5} pincer-like⁶ and mixed phosphines^{7–9} as ligands for transition metals.^{10,11} This upsurge in silylphosphine chemistry has led not only to a number of important discoveries in fundamental reaction

steps¹² but also to advances in their employment as catalysts¹³ and use in materials science. For example, Tobita has informed of a Ru catalyst for alkene hydrogenation bearing a nonspectator Si₂O₂P ligand which exhibits interconversion between η²-H–Si and silyl functions.¹⁴ Turculet successfully employed Pd and Pt silyl pincer complexes for the efficient catalytic conversion of CO₂ to methane.¹⁵

Specifically in the field of catalysis, the design of new catalysts for important transformations such as hydrosilylation^{16–20} and dehydrogenative silylation^{21–23} compels deep knowledge of the fundamental reaction steps often invoked including Si–H bond activation²⁴ and M–Si²⁵ and Si–C²⁶ bond formation. On the other hand, Rh and Ir complexes are the preferred catalysts in a number of chemical transformations owing to their high efficiency, high functional group tolerance^{27–29} and broad substrate scope.^{30–33} In particular, Rh and Ir complexes bearing pincer ligands undergo remarkably facile Si–H bond activation often invoked to be partly due to their ability to support high oxidation states^{12,18,34} as well as to the various coordination modes adopted by the ligands on the metal center.^{35–39}

^aCentro de Investigaciones Químicas, Instituto de Investigación en Ciencias Básicas y Aplicadas, Universidad Autónoma del Estado de Morelos, Avenida Universidad 1001, Col. Chamilpa, Cuernavaca, Morelos, C. P. 62209, México. E-mail: vmontiel@uaem.mx

^bCNRS, LCC (Laboratoire de Chimie de Coordination), 205 route de Narbonne, BP 44099, F-31077 Toulouse Cedex 4, France. E-mail: sylviane.sabo@lcc-toulouse.fr

^cUniversité de Toulouse, UPS, INPT, F-31077 Toulouse Cedex 4, France

^dFacultad de Química, Universidad Nacional Autónoma de México, Mexico City 04510, México

† Electronic supplementary information (ESI) available: Additional spectroscopic (NMR and IR) characterisation of all complexes and X-ray data of compounds **1**, **3Rh**, **3Ir**, **4Rh** and **5Rh**. CCDC 1533806–1533808, 1533794 and 1533878. For ESI and crystallographic data in CIF or other electronic format see DOI: 10.1039/c7dt00727b

Stobart,^{40–44} Sola⁴⁵ and other workers including ourselves^{46,47} have proved that incorporation of a Si–H function into a semi-rigid polydentate phosphine template leads to very pronounced stereoelectronic control over substrate entry, binding and release on a coordinatively unsaturated transition-metal centre. In light of the above, we sought to investigate the coordination ability to Rh and Ir towards a family of semirigid benzylsilyl phosphines bearing a single phosphorus atom and a varying number of potentially coordinating Si–H moieties.

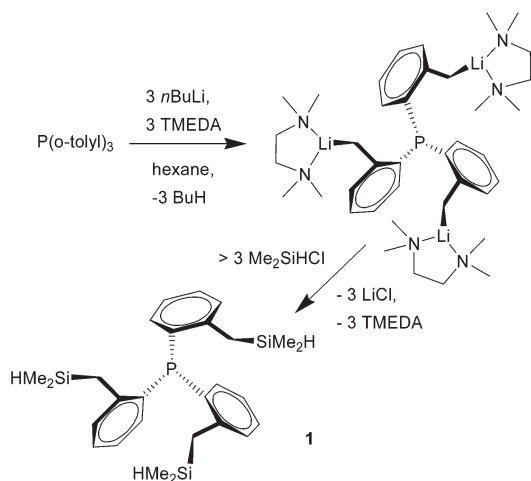
Results and discussion

Synthesis of tris(*o*-benzyl dimethylsilyl)phosphine, **1**

Compound **1** was synthesized following the method previously reported for the synthesis of bis(*o*-benzyl dimethylsilyl)phenylphosphine.⁴⁶ Polyolithiation of tris(*o*-tolyl)phosphine in the presence of TMEDA and subsequent quenching with excess HSiMe₂Cl led after work up to pure **1** as a white solid in excellent yield (91%, Scheme 1).

The main features of **1** in the ¹H NMR spectrum at 298 K in toluene-*d*₈ are the Si hydride resonance at δ 4.28 which exhibits a doublet of nonets multiplicity (³J_{H–H} 3.5 Hz, ⁵J_{P–H} 1.5 Hz) with ²⁹Si satellites and a ¹J_{Si–H} of 189 Hz (Fig. 1). The fine structure is due to the presence of six neighbouring hydrogens of the two methyl groups on silicon and one methylene group which couple equally affording a nonet pattern. The additional doublet splitting is due to coupling to the phosphorus nucleus.

The methyl protons appear as a sharp doublet at δ 0.15 (³J_{H–H} 3.5 Hz), while the benzylic resonance centred at δ 2.42 is broad, indicating deviation from the ideal C₃ symmetry. Indeed, **1** shows dynamic behaviour as evidenced by variable temperature NMR studies (Fig. 1 and the ESI†). Determination of Δ*G*[‡] values indicates that an energy barrier of *ca.* 54 kJ mol^{–1} is overcome at high temperatures in accordance



Scheme 1 Synthesis of tris(*o*-benzyl dimethylsilyl)phosphine, **1**.

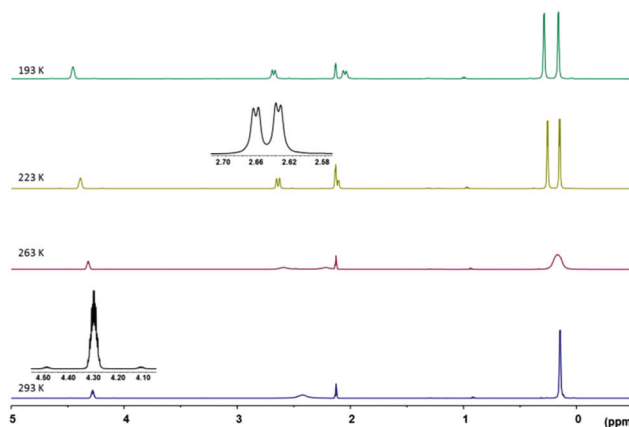


Fig. 1 Stack plot of the ¹H NMR spectra (C₇D₈) of compound **1** recorded between 293 and 193 K.

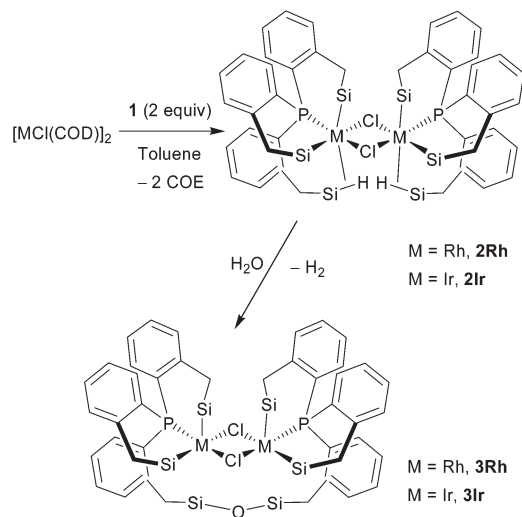
with the adoption of a C₃ molecular symmetry, a rigid configuration (C₁) being adopted at low temperatures due to hindered rotation around the Si–C bonds (ESI†). This is in accordance with the bulkiness of compound **1** which is expected to be even bulkier than its parent precursor tris(*o*-tolyl)phosphine which has a Tolman cone angle of 194°.⁴⁸

A singlet close to δ –27 in the ³¹P{¹H} NMR spectrum of **1** is observed at all temperatures while in the ¹³C{¹H} NMR spectrum the benzylic carbons appear as a doublet at δ 23.4 (³J_{P–C} 19.3 Hz) and the methyl carbons as a singlet at δ –4.25.

The ²⁹Si signal at δ –12.1 features a ¹J_{Si–H} coupling constant of 189 Hz. No coupling constant between the phosphorus and the silicon nuclei was measured, therefore ruling out the possibility of any intramolecular phosphorus–silicon bond interaction despite the relatively rigid structure of **1** which could account for a decrease in the distance between these two atoms. Despite the poor quality of the measurement, X-ray diffraction analysis confirms the proposed structure (see the ESI†).

Synthesis of complex **2Rh**

Room temperature addition of **1** to the rhodium dimer [RhCl(COD)]₂ in toluene-*d*₈ in a 2 : 1 molar ratio afforded gas evolution and isolation after work up of an off-brown solid in a very good yield (83%) (Scheme 2). Elemental analysis and spectroscopic data are in accordance with the formula [ClRh(SiMe₂CH₂-*o*-C₆H₄)₂P(*o*-C₆H₄-CH₂SiMe₂H)]₂, **2Rh**. The symmetrical dinuclear species is characterized by a ³¹P{¹H} doublet at δ 27.8 with a ¹J_{RhP} 154 Hz in accordance with a Rh(III).^{49,50} Variable temperature 2D-multinuclear NMR experiments were in particular diagnostic of the existence of two types of SiMe₂CH₂-*o*-C₆H₄ fragments in a 2 : 1 ratio; one type comprising two of these fragments forming a six-membered ring through silyl coordination to the rhodium centre and a second type displaying a rather weak agostic Si–H coordination mode to Rh. The ¹H NMR spectrum at room temperature shows a broad doublet at δ 2.56 exhibiting a small *J*_{H–Rh} of 6.4 Hz which is assigned to the agostic Si–H with satellites and



Scheme 2 Synthesis of complexes **2** and **3**. Methyl groups on Si are omitted for clarity.

an apparent $J_{\text{Si-H}}$ of 51 Hz. The complex is fluxional as illustrated by the methyl resonances which are characterized at room temperature by a singlet at δ 0.32 and a broad signal at δ 0.56 in a 2 : 1 ratio. In the slow exchange regime at 223 K, the singlet resolves into four singlets at δ 1.22, 0.90, 0.59 and 0.36 whereas the broad signal resolves into two slightly broad signals at δ 0.54 and δ -0.38, each integrating for a single methyl (Fig. 2). The activation parameters for the exchange of the diastereotopic methyl hydrogens were estimated in the range ΔG^\ddagger 52–55 kJ mol⁻¹ (at $T_{\text{c est}}$ 263 K).

Additionally, the methylene benzylic hydrogens observed at room temperature as a very broad signal at δ 2.15 resolve in the slow exchange regime at 223 K, into five signals, one of them with an integral value double that of the value of the other four. The calculated energy for activation is 52 kJ mol⁻¹ with an estimated coalescence temperature of 273 K. The similarity of these values for both methyl and benzylic hydrogens

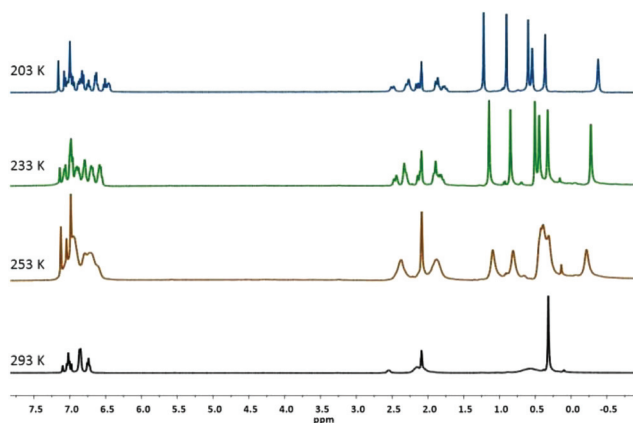


Fig. 2 Stack plot of the ¹H NMR spectra of **2Rh** recorded between 293 and 203 K.

is to be noted. They are also very similar to the ligand precursor **1** despite complexation which implies that the main contribution to the activation energy is rotation around the Si–C bonds.

At 223 K, the ¹³C{¹H} NMR spectrum shows six methyl carbon sharp singlets between 10.1 < δ < -4.8 while three doublets are observed for the benzylic methylene carbons. Conducting a ¹³C{¹H}{³¹P} measurement allows the assignment of the methylene attached to the agostic Si–H at δ 22.8.

At room temperature, despite the use of a variety of sequences, we were unable to detect any reliable ²⁹Si NMR signal. However, at 223 K, the ²⁹Si DEPT{¹H} spectrum shows three signals at δ 57.0 (dd, ¹J_{Si-Rh} 37, ²J_{Si-P} 11 Hz), δ 52.9 (dd, ¹J_{Si-Rh} 39, ²J_{Si-P} 12 Hz) and δ -10.5 (s, $w_{1/2}$ 10 Hz) as confirmed with {³¹P} decoupling.

Additionally, by ²⁹Si DEPT{³¹P}, the signal at δ -10.5 displays a ¹J_{Si-H} coupling constant of 149 Hz which should be compared to the value of 189 Hz obtained for free ligand **1** under the same conditions (Fig. 3). This value is in agreement with a weakly activated agostic Si–H interaction^{11,46,47,51} and in line with the chemical shift of δ 2.56 observed in the ¹H NMR experiment, shifted to a higher field with respect to ligand **1** but still not in the usual metal hydride negative chemical shift range. More information was gathered from ²⁹Si–¹H HMQC {³¹P} experiments (see Fig. 4, Experimental section and the ESI† for full assignment at 293 K and 223 K). The fact that at room temperature, when there is no distinguishable ²⁹Si signal, a $J_{\text{Si-H}}$ value of ca. 50 Hz was determined by ¹H NMR while it was ca. 150 Hz at the slow exchange regime, implies that at RT, the single hydrogen nucleus is in fact in exchange between the three Si atoms: an average value ¹J_{Si-H}/3 is measured due to exchange between H connected to ²⁹Si isotopes with H connected to ²⁸Si isotopes where ¹J_{Si-H} is zero. When the exchange process is blocked, the hydride only coordinates to one silicon providing an agostic function and the corresponding coupling constant is close to 150 Hz.⁴⁶

It is remarkable that the silyl signals at δ 57.0 and at δ 52.9 show similar coupling constants to rhodium (ca. 38 Hz) in agreement with the direct bond between the Si and Rh atoms.

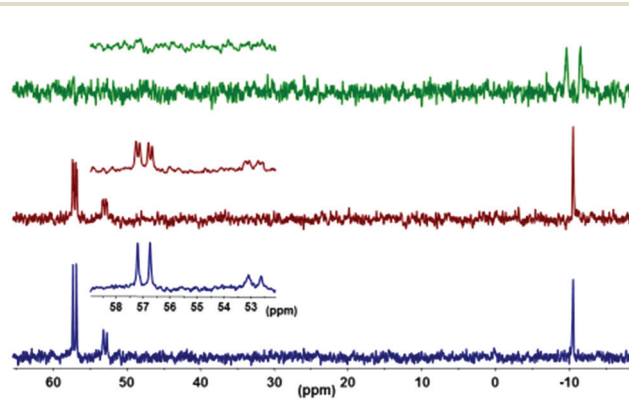


Fig. 3 Stack plot of the ²⁹Si DEPT spectra (223 K) of **2Rh** with different decoupling schemes. Top: ²⁹Si DEPT {³¹P} without ¹H decoupling, middle: ²⁹Si DEPT {¹H} and bottom: ²⁹Si DEPT {¹H}{³¹P}.

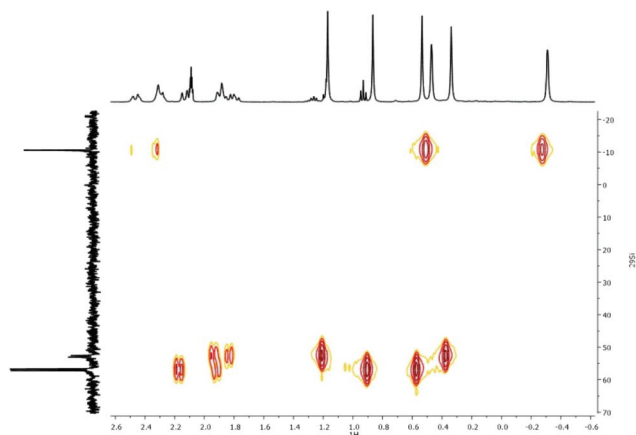


Fig. 4 HMQC ^{29}Si - ^1H NMR spectrum for **2Rh** at 223 K.

In contrast, the $J_{\text{Si-Rh}}$ coupling constant for the third silicon nucleus can be estimated to be less than 10 Hz as inferred from the $w_{1/2}$ value of the corresponding signal.

Observation of a signal in the ^{103}Rh NMR spectrum (Fig. 5) at a chemical shift of δ -8738 (223 K), shifted to a higher field in comparison with $[\text{RhCl}(\text{COD})]_2$ which appears at δ -7212, is comparable to the case of $[\text{Rh}(\text{H})_2(\text{SiMe}_2\text{Ph})(\text{PMe}_3)_3]$ where the complex shifts over 1000 ppm to the higher field upon complexation in relation to the rhodium precursor.⁵²

Monitoring the reaction in a Young's NMR tube allows the detection of released molecular hydrogen and COD upon addition of **1** to $[\text{RhCl}(\text{COD})]_2$. Gradual consumption of H_2 leads to the formation of COE upon a period of 2 hours. Hence, in conclusion upon reaction, the dinuclear structure with chloro bridges is maintained while COE is released thanks to COD hydrogenation. This leads to the formation of the disilyl complex **2Rh** with the third silicon atom of the initial ligand **1** forming a rather weak $\text{Rh}(\eta^2\text{-SiH})$ interaction, the rhodium centre achieving an 18 electron configuration.

In light of the results obtained from the reactivity of $[\text{RhCl}(\text{COD})]_2$ with the trisbenzylsilanephosphine **1** we turned to study its coordination towards the Ir analogue.

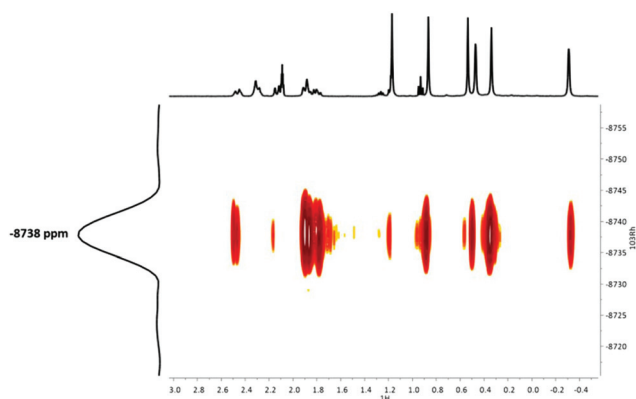


Fig. 5 HMQC ^{103}Rh - ^1H of **2Rh** at 223 K.

Synthesis of compound **2Ir**

Compound **2Ir** was synthesized from the reaction of $[\text{IrCl}(\text{COD})]_2$ and ligand **1** in a 1:2 molar ratio in pentane at room temperature. A yellow solid was isolated after work up in quantitative yield (97%). The gathered spectroscopic data are in accordance with the proposed formula shown in Scheme 2. At room temperature, the ^1H NMR recorded in C_6D_6 exhibits two methyl group resonances as two singlets at δ 0.53 and 0.41 while the benzylic methylene hydrogens appear as a doublet at δ 2.13 (d, $^2J_{\text{H-H}}$ 14 Hz) and a doublet of doublets resonance at δ 2.05 (dd, $^2J_{\text{H-H}}$ 14 Hz, $^4J_{\text{P-H}}$ 3 Hz). The Si-H resonance is shown at δ 0.55 as a broad signal with well-resolved ^{29}Si satellites and an apparent $J_{\text{Si-H}}$ coupling of 42 Hz. In comparison to compound **2Rh**, the agostic Si-H moieties are slightly more activated in **2Ir** as indicated by the value of the coupling constant $J_{\text{Si-H}}$ and the more shielded chemical shift. In contrast to **2Rh**, complex **2Ir** shows two sets of equally-integrating methyl and methylene hydrogens implying that at room temperature the three silicon atoms must be equally sharing the non-classical hydrogen resulting in only two magnetically different environments for both the methyl and methylene hydrogens. This situation would differ to the one proposed for complex **2Rh** in which the hydrogen should be jumping between the three silicons at room temperature but be bound to only one at a time.

In the $^{13}\text{C}\{^1\text{H}\}$ NMR spectrum, two methyl carbon signals are observed as singlets at δ 2.22 and 2.93 while a unique methylene carbon is observed at δ 27.6 as a doublet due to a $^3J_{\text{P-C}}$ (11 Hz). In the $^{31}\text{P}\{^1\text{H}\}$ a singlet signal appears at δ 0.21, thus quite shifted with respect to **2Rh**. The ^{29}Si NMR spectrum measured at 293 K (toluene- d_8) shows only one signal at δ 10.0 correlating with the methylene, methyl and Si-H resonances thus indicating a fast exchange between the three silicon atoms. Upon lowering the temperature down to 180 K, we were unable to block the exchange process, all the signals becoming broad. This is in contrast to the rhodium case for which decoalescence was observed leading to an arrested agostic Si-H interaction characterized by a ^{29}Si resonance at δ -10.5 with a $^1J_{\text{Si-H}}$ of 149 Hz and showing a reduced $J_{\text{Si-Rh}} < 10$ Hz. In the solid state, the IR spectrum of **2Ir** shows the ν_{IrHSi} vibration mode at 2019 cm^{-1} . Attempts at obtaining crystals suitable for X-ray diffraction analysis failed in our hands due to slow decomposition of **2Ir** in solution (see the ESI †).

Synthesis of complex **3Rh**

Attempts at obtaining crystals of complex **2Rh** were unsuccessful. Instead, after days in solution, complex **2Rh** reacts with adventitious water present in the solvent generating complex **3Rh** (Scheme 2), a species of the formula $[(\mu^2\text{-Cl})_2\text{-Rh}_2(\text{SiMe}_2\text{CH}_2\text{-}o\text{-C}_6\text{H}_4)_2\text{P}(o\text{-C}_6\text{H}_4\text{-CH}_2\text{SiMe}_2\text{OSiMe}_2\text{CH}_2\text{-}o\text{-C}_6\text{H}_4)\text{P}(\text{SiMe}_2\text{CH}_2\text{-}o\text{-C}_6\text{H}_4)_2]$. This was confirmed by adding distilled water to a C_6D_6 solution of **2Rh**. Thus, **3Rh** formally results from addition of an O atom to complex **2Rh**, with loss of the agostic interactions $\text{Rh}(\eta^2\text{-SiH})$ and dihydrogen evolution.

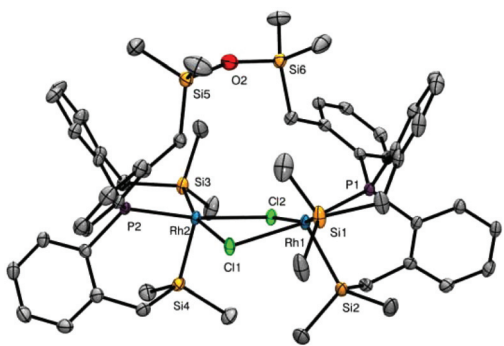


Fig. 6 X-ray diffraction structure of compound **3Rh** with thermal ellipsoids at 30% probability. Selected bond lengths (Å) and angles (°): Rh1–Si1 2.2921(8), Rh1–Si2: 2.288(1), Rh2–Si3 2.2948(8), Rh2–Si4 2.2887(9), Rh1–P1 2.2329(7), Rh2–P2 2.2426(8), Si1–Rh1–Si2 88.37(3), Si3–Rh2–Si4 92.06(3), Si1–Rh1–Cl2 164.66(3), Si3–Rh2–Cl1 166.52(3).

Yellow crystals appropriated for X-ray diffraction analysis were grown from toluene/diethylether (Fig. 6). The collection parameters are collected in Table 1. The molecular structure shows a symmetrical dirhodium dichloride bridged species with a third bridging ligand. The phosphorus and two silicon atoms are coordinated to each Rh centre while the third silicon atoms forms a new Si–O–Si bridging fragment. Each rhodium atom is thus pentacoordinated with a slightly distorted square pyramidal geometry.⁵³ ‡ Around each Rh centre, the apical position *trans* to a vacant site is occupied by the strongest *trans* influence ligand, Si, while the other Si is disposed *trans* to π -donor Cl.^{54,55} The four Rh–Si bond distances are approximately equal at *ca.* 2.29 Å.⁵⁶

The NMR spectra of the crystals were acquired in C_6D_6 . At ambient temperature, in contrast to **2Rh**, the 1H NMR spectrum of **3Rh** shows six singlet signals for the methyl groups and six diastereotopic methylene hydrogen signals indicative of hindered rotation around the Si–O–Si bridge. In the $^{31}P\{^1H\}$ NMR spectrum, a doublet signal at δ 26.8 reflecting the coupling to rhodium (J_{Rh-P} 158 Hz) highlights the equivalence of the two phosphorus atoms and endorses the high symmetry of the molecule.

The $^{29}Si\text{--}^1H$ HMQC NMR experiment (Fig. 7) displays three Si signals. They are observed at δ 5.17, 42.0 and 67.0 in **3Rh** which should be compared to δ –10.5, 52.9 and 57.0 in **2Rh**. Thus a change of *ca.* 10 ppm to a lower field except for the siloxane silicon (δ 5.17) which shifts slightly more. The chemical shift of rhodium also shifts to a lower field from δ –8738 to –8417 ppm.

Synthesis of compound **3Ir**

Keeping solutions of **2Ir** in very dry solvents (dried over potassium mirror) led after a few days to decomposition into

‡ Applying Konno's equation to **3Rh** gives χ values of 0.15 and 0.16; to **4Rh** two values of 0.35; to **5Rh** 0.88 and to **3Ir** 0.15 and 0.18. Thus, for **3Rh**, **4Rh** and **3Ir** the geometry is closer to square pyramidal (ideal value $\chi = 0$) and for **5Rh** it is closer to trigonal bipyramidal geometry (ideal value $\chi = 1$).

unknown species. However, when adventitious water was present, as in the case of the rhodium analogue, **2Ir** was transformed into complex **3Ir** featuring a siloxane bridge. As in the case of the Rh analogue, deliberate addition of degassed deionized water to a C_6D_6 solution of **2Ir** led to the formation of **3Ir** and H_2 . The NMR spectra of **3Ir** are analogous to those of **3Rh**. The $^{31}P\{^1H\}$ NMR (C_6D_6) singlet is at δ –4.54, shifted to a higher field with respect to **3Rh**. In the 1H NMR spectrum, six singlet signals are assigned to the six inequivalent methyl groups, while again six signals, three doublets and three doublets of doublets with additional phosphorus coupling are observed for the inequivalent benzylic hydrogens. **3Ir** is characterized by three ^{29}Si NMR signals at δ 24.1, 5.1 and 3.5 in the HMBC $^{29}Si\text{--}^1H$ spectrum in toluene- d_8 .

Red-orange complex **3Ir** crystallizes from benzene/hexane mixtures giving appropriate crystals for X-ray diffraction analysis (ESI†). The molecular structure (Fig. 8) confirms a dimeric structure with two iridium centres each coordinated to a modified ligand **1** through the phosphorus and two silicon atoms. The third Si atom is again forming part of a Si–O–Si moiety spanning over the two Ir centres together with two Cl bridges.

The structure is very similar to that previously discussed for **3Rh** also exhibiting a square pyramidal geometry only slightly deviated from the ideal one.⁵³ ‡ Once again the strong *trans* influence of Si is responsible for one of these atoms resting on the apical position of the square pyramidal while a second is disposed *trans* to π -donor Cl on the equatorial base.^{57,60,61}

There are only a few literature precedents for the formation of siloxane bridges upon reaction with adventitious water. A siloxane-bridge on a Pt system bearing a PSiP ligand was described by Milstein as a result of Si–H oxidation.⁵⁸ Tilley reported on the addition of O–H across a Ir–Si bond of a dihydride silylene complex resulting in a trihydride siloxane-bridge dimer.⁵⁹ Interestingly, formation of the siloxane bridge upon retention of the unsaturation at a Pt cationic system was observed by Ozerov.⁷ Substituted halo-silyl cyclopentadienyl complexes also react with water to produce the corresponding siloxane bridge.⁶⁰ Finally, it is worth stressing that compound **1** on its own does not react with H_2O even in the presence of its large excess (up to 3000 molar excess).

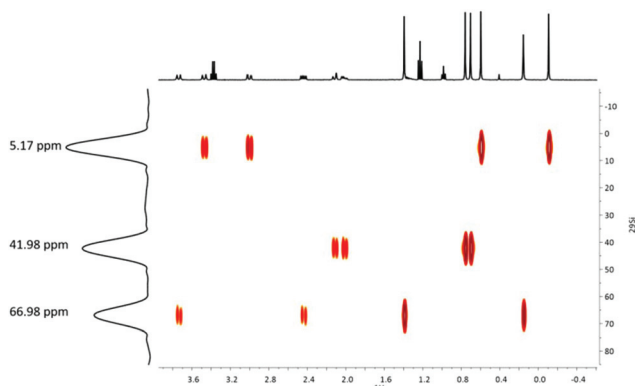
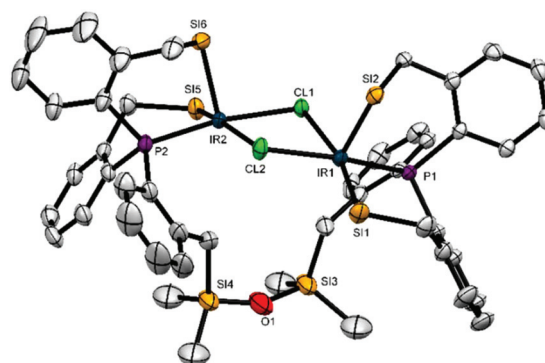
Synthesis of complex **4Rh**

Room temperature addition of $PhP\{(o-C_6H_4)CH_2SiMe_2H\}_2$ instead of **1** to $[RhCl(COD)]_2$ in benzene in a 2 : 1 molar ratio afforded gas evolution, and after work up, isolation of a yellow solid in a very good yield (78%) (Scheme 3). The solid was analysed by elemental analysis and solid state NMR spectroscopy as it turned out to either react or be insoluble in all the available deuterated solvents for solution studies. However, crystals suitable for X-ray diffraction analysis could be grown from hexane solutions. All the data are in agreement with the formulation $[\mu\text{-Cl-Rh}(\text{SiMe}_2\text{CH}_2\text{-}o\text{-C}_6\text{H}_4)_2\text{PPh}]_2$, (**4Rh**) as shown in Scheme 3.

The molecular structure obtained by X-ray diffraction analysis (Table 1, Fig. 9) shows a dimeric structure with two chlor-

Table 1 Crystal data and details of the structure determination of compounds **3Rh**, **4Rh**, **5Rh** and **3Ir**

Compound	3Rh	4Rh	5Rh	3Ir
Formula	C ₅₄ H ₇₂ Cl ₂ OP ₂ Rh ₂ Si ₆ C ₄ H ₈ O	C ₄₈ H ₅₈ Cl ₂ P ₂ Rh ₂ Si ₄ 2(C ₆ H ₆)	C ₄₂ H ₄₄ ClP ₂ RhSi ₂ 3(C ₄ H ₈ O)	C ₅₄ H ₇₂ Cl ₂ Ir ₂ OP ₂ Si ₆
Formula weight	1318.44	1242.18	1021.56	1422.89
Crystal system	Monoclinic	Monoclinic	Monoclinic	Monoclinic
Space group	<i>P2₁/n</i>	<i>P2₁/c</i>	<i>C2/c</i>	<i>P2₁/c</i>
<i>a</i> , <i>b</i> , <i>c</i> [Å]	18.7944(11), 13.7302(8), 23.8886(13)	11.74490(13), 21.9235(2), 12.01200(13)	20.6490(6), 17.2473(4), 13.9539(4)	13.7427(3), 24.3307(5), 20.5811(4)
α , β , γ [°]	90, 94.744(3), 90	90, 108.2606(12), 90	90, 91.939(3), 90	90, 99.626(2), 90
<i>V</i> [Å ³]	6143.4(6)	2937.20(6)	4966.7(2)	6784.8(2)
<i>Z</i>	4	2	4	4
<i>d</i> (calc.) [g cm ⁻³]	1.425	1.405	1.366	1.393
μ [mm ⁻¹]	0.833	6.956	0.553	4.182
<i>F</i> (000)	2736	1280	2144	2824
Crystal size [mm]	0.16 × 0.09 × 0.02	0.03 × 0.09 × 0.13	0.09 × 0.11 × 0.14	0.2 × 0.34 × 0.42
Temperature (K)	100(2)	100	100	130(2)
Radiation [Å]	MoK α	CuK α	Mok α	Mok α
θ min–max [°]	0.71073	1.54184	0.71073	0.71073
θ min–max [°]	2.57, 26.37	4.0, 72.7	2.8, 29.1	3.405, 29.592
Dataset	–23 : 23, –17 : 17, –29 : 29	–14 : 12; –27 : 25; –9 : 14	–26 : 27; –21 : 23; –17 : 18	–19 : 18, –33 : 33, –27 : 25
Tot., uniq. data, <i>R</i> (int)	240 484, 12 549, 0.0488	11 269, 5700, 0.022	20 468, 5972, 0.026	105 030, 17 406, 0.0453
Data/restraints/parameters	12 549/0/663	5700/0/320	5972/60/289	17 406/36/615
Goodness of fit on <i>F</i> ²	1.12	1.02	1.06	1.08
Final <i>R</i> indices [<i>I</i> > 2 σ (<i>I</i>)]	<i>R</i> ₁ = 0.0318, <i>wR</i> ₂ = 0.0763	<i>R</i> ₁ = 0.0271, <i>wR</i> ₂ = 0.0716	<i>R</i> ₁ = 0.0341, <i>wR</i> ₂ = 0.0833	<i>R</i> ₁ = 0.0344, <i>wR</i> ₂ = 0.0684
<i>R</i> indices (all data)	<i>R</i> ₁ = 0.0420, <i>wR</i> ₂ = 0.0849	<i>R</i> ₁ = 0.0301, <i>wR</i> ₂ = 0.0737	<i>R</i> ₁ = 0.0399, <i>wR</i> ₂ = 0.0868	<i>R</i> ₁ = 0.0538, <i>wR</i> ₂ = 0.0781
Largest diff. peak and hole (e Å ⁻³)	1.23, –0.80	1.01, –0.67	1.05, –0.87	2.30, –1.57

**Fig. 7** ²⁹Si–¹H HMQC NMR spectrum for **3Rh** at 223 K.**Fig. 8** X-ray diffraction structure of compound **3Ir** with thermal ellipsoids at 50% probability. Selected bond lengths (Å) and angles (°): Ir1–Cl1 2.5877(10), Ir2–Cl2 2.5721(11), Ir1–Cl2 2.3904(10), Ir2–Cl1 2.3811(9), Ir1–Si1 2.3050(12), Ir2–Si5 2.3090(13), Ir1–Si2 2.2937(12), Ir2–Si6 2.2914(13), Ir1–P1 2.2203(10), Ir2–P2 2.2274(11), Ir1–Cl1–Ir2 97.39(3), Ir2–Cl1–Ir1 97.39(3), Ir1–Cl2–Ir2 97.57(4), P1–Ir1–Si2 90.73(4), P1–Ir1–Si1 91.06(4), Si1–Ir1–Si2 92.22(5), Si2–Ir1–Cl2 97.16(4), Si1–Ir1–Cl1 167.09(4).

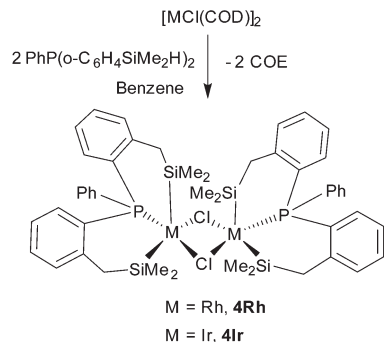
ide atoms bridging the rhodium centres. Each rhodium atom has a ligand coordinated through the phosphorus and two silicon atoms in a facial mode. In this case, the geometry around the rhodium centre, at least in the solid state, can be best described by applying Konno's equation as a slightly distorted square pyramid with the apical position being occupied by one of the silicon atoms.⁵³ ‡ The apical Rh–Si bond distances are only slightly shorter (2.2825(6) Å) than the corresponding equatorial Rh–Si bonds (2.2960(6) Å) as expected from the lack of a *trans* ligand in the former case. The Rh–Rh bond distance is 3.7010 Å excluding the existence of a metal–metal bond.⁶¹ Selected bond distances and angles are shown in Fig. 9.

The solid state ¹H MAS NMR spectrum of compound **4Rh** shows three signals which can be assigned to the methyl, benzylic and aromatic hydrogens. The ¹³C CP MAS spectrum

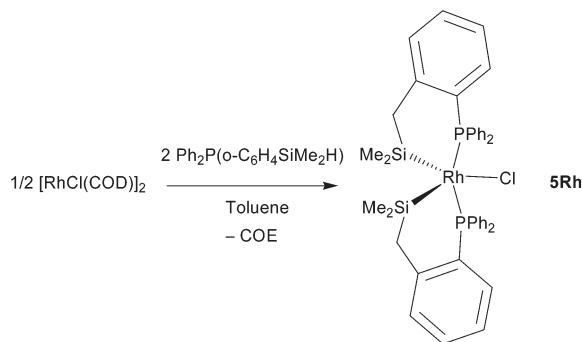
gives more information by exhibiting three methyl carbon resonances and two benzylic carbon signals. In the ³¹P NMR spectrum, a unique signal is observed at δ 45.3 while in the ²⁹Si NMR spectrum two signals at δ 54.9 and 64.9 are assigned to the two distinct Si nuclei. We believe that the solid state NMR data are fully consistent with the X-ray structure determined for complex **4Rh**.

Synthesis of compound **4Ir**

Compound **4Ir** was synthesized in an analogous fashion to **4Rh**. The yellow crystalline solid, formulated as [μ -Cl-Ir



Scheme 3 Synthesis of complexes 4.



Scheme 4 Synthesis of complex 5Rh.

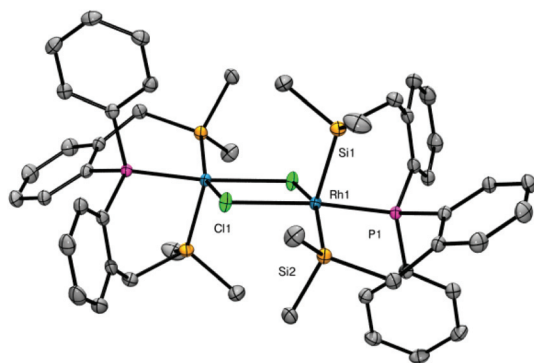


Fig. 9 X-ray diffraction structure of compound **4Rh** with thermal ellipsoids at the 50% probability level. Selected bond lengths (Å) and angles (°): Rh1–Si1 2.2825(6), Rh1–Si2 2.2960(6), Rh1–Cl1 2.4160(5), Rh1–P1 2.2075(5).

$(\text{SiMe}_2\text{CH}_2\text{-}o\text{-C}_6\text{H}_4)_2\text{PPh}_2$, was characterized by solid state NMR with a broad signal at δ 11.8 in the ^{31}P CP MAS spectrum, and two broad signals at δ 22.7 and 13.8 in the ^{29}Si CP MAS spectrum assigned to two distinct Si nuclei.

Synthesis of complex 5Rh

When employing the monosilicon-substituted diphenylphosphine compound $\text{Ph}_2\text{P}(o\text{-C}_6\text{H}_4)\text{CH}_2\text{SiMe}_2\text{H}$, the room temperature addition to $[\text{RhCl}(\text{COD})]_2$ in toluene in a 4 : 1 molar ratio afforded gas evolution and isolation after work up of an off-brown solid in a very good yield (78%) (Scheme 4). Full characterization of the compound allows us to formulate it as the 16-electron mononuclear complex $[\text{RhCl}(\text{SiMe}_2\text{CH}_2\text{-}o\text{-C}_6\text{H}_4\text{-PPh}_2)_2]$, **5Rh**. This d^6 compound is analogous to the previously reported $[\text{RhCl}(\text{SiMe}_2\text{-(CH}_2)_2\text{-PPh}_2)_2]$ by Stobart as a result of the reaction of the same rhodium precursor with the alkyl bridged silylphosphine $\text{Ph}_2\text{P}(\text{CH}_2)_2\text{SiMe}_2\text{H}$.⁴⁴ Complex **5Rh** shows a unique signal at δ 23 in the $^{31}\text{P}\{^1\text{H}\}$ NMR spectrum with a doublet multiplicity due to coupling to rhodium $^1J_{\text{Rh-P}}$ 117 Hz indicating the high symmetry in the molecule.

The diastereotopic benzylic hydrogens appear as two higher order signals close to δ 2, diastereotopicity being conferred because of restricted rotation as a consequence of chelation.

All coupling constants and assignments were confirmed by 2D and decoupling NMR experiments.

More interestingly, a ^{29}Si DEPT $\{^{31}\text{P}\}$ experiment of complex **5Rh** shows only one doublet at δ 54.4 ($^1J_{\text{Si-Rh}}$ 33 Hz). Broad band coupling of ^{31}P allows for the observation of a doublet of triplet resonance with couplings of silicon to rhodium and phosphorus (td, $^1J_{\text{Si-Rh}}$ 33 Hz, $^2J_{\text{Si-P}}$ 12 Hz). These experiments confirm the presence of two equivalent silylphosphine chelating ligands in the molecule in accordance with a highly symmetrical molecule.

A suitable crystal for X-ray diffraction analysis was grown from a concentrated THF solution. The collection parameters are collected in Table 1. The molecular structure shown in Fig. 10 confirms a highly symmetric monomeric structure resulting from coordination of two P,Si chelating ligands. The coordination geometry around rhodium is best described as a distorted trigonal bipyramid after applying Konno's treatment to the angles around Rh.⁵³ ‡ The two phosphorus atoms occupy the axial positions while the silicon atoms are disposed in the equatorial base.

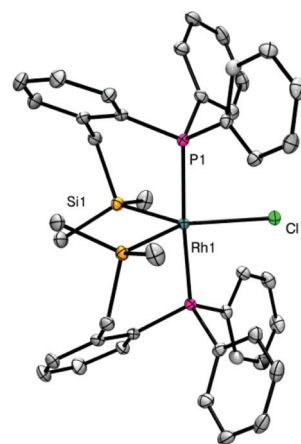


Fig. 10 X-ray diffraction structure of compound **5Rh** with thermal ellipsoids at 50% probability. Selected bond lengths (Å) and angles (°): Rh–Si1 2.3415(6), Rh–P1 2.3478(5), Si1–Rh–Si1a 84.76(2), P1–Rh–P1a 175.93(2), Cl–Rh–Si1 137.62(2).

Although most d^6 ML_5 compounds are known to adopt a square-pyramidal structure with the apical site being occupied by the largest *trans* influence ligand, it is known that some others adopt a distorted trigonal bipyramid structure when bearing a π -donor group, even if very weak ones like chlorine and fluoroalkoxy groups.⁵⁷ In fact, this last class of compounds exhibit a very acute angle between the two groups opposite to the π -donor ligand which cannot be explained by steric reasons. This acute angle maximizes the electron-donation of the π -donor ligand contributing to a partial metal-ligand multiple bond. Indeed, **5Rh** displays an acute Si1–Rh–Si2 angle of $84.75(3)^\circ$ resulting in larger Cl–Rh–Si angles in agreement with previous theoretical work.^{57,62} The rest of the bond angles and distances are within the reported parameters for analogous species.

Conclusions

In this study, we have further extended our method for preparing polyfunctional phosphinosilane compounds. We have reported the synthesis in excellent yield of the tris-(*o*-benzyl-dimethylsilyl)phosphine, **1**, featuring three Si–H bonds, being thus able to act as a tetradentate ligand. By studying its coordination behaviour towards the rhodium and iridium $[MCl(COD)]_2$ precursors, we were able to show that the denticity of this new ligand can be modified. In the resulting complexes **2**, a tetradentate ligation was achieved through the coordination of phosphorus, two silyl moieties resulting from the activation of two Si–H bonds, and a third Si atom stabilizing the metal centre *via* an agostic Si–H coordination mode. The dimeric central core is preserved and the metal exhibits an oxidation state of III. In the rhodium case, the agostic Si–H interaction is rather weak as evidenced by ^{29}Si NMR studies at low temperature with a reduced $^1J_{Si-H}$ coupling constant of 149 Hz in comparison to those of the free ligand (189 Hz). In the iridium case, a more shielded 1H resonance and an estimated value of 126 Hz (3×42 Hz) are in agreement with a slightly higher degree of activation. The isolation and characterization of complexes **2** proved to be challenging due to their high reactivity to traces of water. The agostic Si–H bonds are indeed readily broken to form a bridging siloxane ligand spanning the two metal centres and resulting in the formation of complexes **3**. When the reaction is carried out with the disubstituted benzylsilylphosphine compound $PhP\{(o-C_6H_4)CH_2SiMe_2H\}_2$, the dimeric central core is also preserved, the metal centers achieving a 16-electron configuration with two distinct silyl groups. Solid state NMR, and particularly ^{29}Si solid state NMR proved to be a valuable tool to better characterize complexes **4** due to their poor solubility. It is worth noting that here the reaction of the phosphinodi(benzylsilane) $PhP\{(o-C_6H_4)CH_2SiMe_2H\}_2$ with the rhodium and iridium precursors leads to Si–H bond breaking whereas a pincer-type ligation is obtained upon reaction with the ruthenium polyhydride $RuH_2(H_2)_2(PCy_3)_2$, thus favouring the coordination through two agostic Si–H bonds.⁴⁶ Finally, the reactivity of the starting

rhodium dimer was probed toward the monosubstituted benzylsilylphosphine compound $Ph_2P(o-C_6H_4)CH_2SiMe_2H$. Here, the dimer core was broken and the corresponding mononuclear complex **5Rh** was isolated and fully characterized including ^{29}Si NMR data in agreement with two equivalent silylphosphine chelating ligands.

We now intend to use this series of benzylsilyl phosphines to explore transition-metal catalysed transformations with a specific focus on the role of the agostic Si–H interactions.

Experimental section

General considerations

All experiments were performed under an argon atmosphere using standard Schlenk methods or in MBraun glove boxes. THF, Et₂O, toluene, hexane and pentane were either dried and distilled from sodium using benzophenone ketyl as an indicator or purified over a MBraun column system. In either case, they were degassed prior to use. Benzene-*d*₆ and toluene-*d*₈ were either degassed *via* three freeze–pump–thaw cycles and stored over molecular sieves or stored over a freshly prepared potassium mirror in an ampoule fitted with a J. Young's valve. $[MCl(COD)]_2$ (M = Rh, Ir) were synthesized according to reported procedures.^{63,64} The other reagents were purchased from Sigma Aldrich and used as received. Nuclear magnetic resonance spectra in solution were recorded on Bruker Avance 300, 400, 500, Varian Inova 400 MHz and Varian NMRS-700 MHz spectrometers. Solid-state NMR experiments were recorded on a Bruker AvanceIII 400 spectrometer equipped with a 3.2 or 4 mm probe. Samples were spun between 6 to 16 kHz at the magic angle using ZrO₂ rotors. For ^{31}P MAS single pulse experiments, small flip angles ($\sim 30^\circ$) were used with recycle delays of 10 s. ^{13}C , ^{29}Si and ^{31}P -CPMAS spectra were recorded with a recycle delay of 2 s and contact times of 2 ms, 3 ms and 2 ms respectively. All chemical shifts for 1H , ^{29}Si and ^{13}C are relative to TMS. ^{31}P chemical shifts were referenced to an external 85% H₃PO₄ sample. Infra-red spectra were recorded on Nicolet 6700 and Bruker Alpha FT-IR spectrophotometers in absorbance (KBr disc, Nujol and solution) and ATR modes. Microanalyses were performed at the Laboratoire de Chimie de Coordination on a PerkinElmer 2400 series II analyzer.

Synthesis of $P\{(o-C_6H_4)CH_2SiMe_2H\}_3$, **1**

The phosphine $P\{(o-C_6H_4)CH_2SiMe_2H\}_3$ was made *in house* from the reaction of three equivalents of $BrMg(o-C_6H_4)CH_3$ and one equivalent of PCl_3 . A THF (5 mL) solution of $Br(o-C_6H_4)CH_3$ (41.6 mmol) was added dropwise to activated Mg (1 g, 41 mmol) and the reaction mixture was left to react at reflux temperature until the full consumption of the activated magnesium. Addition of PCl_3 (1.2 mL, 13.9 mmol) and stirring for 24 h left a yellow solution and a white precipitate of $MgBrCl$ which was separated by filtration. To the solution, ice (2 g) was added followed by 100 mL of a 0.5 M aqueous NH_4Cl solution. The product was extracted three times with 100 mL of ethyl

ether using a separating funnel. The ethereal phase was collected, dried over MgSO₄ and finally evaporated to dryness. The yellowish powder was further purified by recrystallization from hot ethanol solutions at 263 K to yield a white solid in 89%, and its purity was verified by m.p. and ¹H and ³¹P NMR. P{(o-C₆H₄)CH₃}₃ (1 g, 3.3 mmol) was dissolved in 30 mL of hexane, and then TMEDA (1.48 mL, 9.9 mmol) and titrated hexane solution of *n*BuLi (3.96 mL, 9.9 mmol) were added. After stirring for 20 h, the bright orange red reaction mixture was cooled to 195 K and excess ClSiMe₂H (3 mL, 27 mmol) was added *via* syringe. The off-white suspension was allowed to warm up to room temperature and kept under stirring for 12 h, after which the solvent was removed by distillation under a reduced pressure. The white solid was dissolved in 15 mL of hexane and recrystallized overnight at 263 K. Yield 91% from P{(o-C₆H₄)CH₃}₃. M.p. 375 K. Anal. Calcd for C₂₇H₃₉PSi₃: C, 67.73; H, 8.21. Found: C, 67.70; H, 8.15. ¹H NMR (C₆D₆, 400 MHz, 293 K): δ 7.04 (tt, ³J_{H-H} 7.7 Hz, ⁴J_{H-H} 1.14 Hz, 3H), 7.01 (m, 6H), 6.82 (t, ³J_{H-H} 7 Hz, 3H), 4.26 (nd, ³J_{H-H} 3.6 Hz, ⁵J_{P-H} 1.8 Hz, ¹J_{Si-H} 189 Hz satellites, 3H), 2.38 (br. s, 6H), 0.08 (d, ³J_{H-H} 3.6 Hz, 18H). ¹³C{¹H} NMR (175 MHz, C₆D₆) δ 145.1 (d, ¹J_{P-C} 26.3 Hz), 134.1 (s), 133.7 (d, ²J_{P-C} 10.5 Hz), 129.0 (d, ²J_{P-C} 5.3 Hz), 128.7 (s), 125.1 (s), 23.4 (d, ³J_{P-C} 19.3 Hz, CH₂), -4.25 (s, CH₃, ¹J_{Si-C} 50.8 Hz, satellites). ³¹P{¹H} NMR (161.9 MHz, C₆D₆) δ -27.0. ²⁹Si{¹H} NMR (75.54 MHz, C₆D₆) δ -12.1 (s). IR (KBr disc) 2119 cm⁻¹ (s, νSi-H), 1247 cm⁻¹ (s, νSi-Me₂), 887 cm⁻¹ (s, ωSi-H).

Synthesis of [Rh₂(μ-Cl)₂P{[η²-(H-SiMe₂)CH₂C₆H₄][(o-C₆H₄)CH₂SiMe₂]}₂], 2Rh

In a Schlenk flask, compound **1** (215 mg, 0.45 mmol) and [RhCl(COD)]₂ (110 mg, 0.22 mmol) were degassed and then dissolved in toluene-d₈ (1.5 mL). The solution was stirred for two hours at room temperature after which it was concentrated and kept overnight at 236 K. The resulting yellow solid was washed twice with 0.5 mL of Et₂O to yield a light brown solid. Yield 83% (91 mg). Anal. Calcd for C₅₄H₇₄Cl₂O₂P₂Rh₂Si₆: C, 52.72; H, 6.06. Found: C, 52.96; H, 6.10. ¹H NMR (300 MHz, C₇D₈, 293 K): δ 7.10 (br. s, 1H, CH), 7.01 (br. m, 3H, CH), 6.86 (br. m, 6H, CH), 6.74 (br. m, 3H, CH), 2.56 (br. d, ¹J_{H-Rh} 6.4 Hz, ¹J_{H-Si} 53.4 Hz from ²⁹Si satellites, 2H, η²-HSi), 2.15 (br. ψt, ²J_{H-H} 16 Hz, 12H, SiCH₂), 0.56 (br. s, 12H, SiCH₃), 0.32 (s, 24H, SiCH₃). ³¹P{¹H} NMR (161.9 MHz, C₇D₈): δ 27.8 (d, ¹J_{P-Rh} 154 Hz). ¹³C{¹H} NMR (100.61 MHz, C₇D₈, 223 K): δ: 146.8 (t, ¹J_{C-P} 12.5 Hz, ²J_{C-Rh} 12.5 Hz, *C*_{ipso}-P), 144.9 (d, ¹J_{C-P} 18.4 Hz, *C*_{ipso}-P Rh-η²(Si-H)), 135.0 (s, *C*_{ipso}-C), 135.0 (s, *C*_{ipso}-C), 131.1 (s, *C*_{ipso}-C), 131.0–130.8 (overlapped higher order m, CH_{aromatic}), 130.7 (d, *J*_{C-P} 4.9 Hz, CH_{aromatic}), 130.5 (d, *J*_{C-P} 8.0 Hz, CH_{aromatic}), 130.4 (d, *J*_{C-P} 5.1 Hz, CH_{aromatic}), 125.5 (d, *J*_{C-P} 6.3 Hz, CH_{aromatic}), 124.6 (m, CH_{aromatic}), 32.1 (d, ³J_{C-P} 18.8 Hz, CH₂), 30.8 (d, ³J_{C-P} 16.2 Hz, CH₂), 22.8 (d, ³J_{C-P} 4.3 Hz, CH₂), 10.1 (s, CH₃), 9.6 (s, CH₃), 5.0 (s, CH₃), 3.9 (s, CH₃), -4.6 (s, CH₃), -4.8 (s, CH₃). DEPT ²⁹Si{¹H} NMR (79.49 MHz, C₇D₈, 223 K) δ: 57.0 (dd, ¹J_{Si-Rh} 36.7 Hz, ²J_{Si-P} 10.9 Hz, Rh-Si), 52.9 (dd, ¹J_{Si-Rh} 38.7 Hz, ²J_{Si-P} 12.3 Hz, Rh-Si), -10.5 (s, *w*_{1/2} 10.3

Hz, Rh-η²(Si-H)). HMQC ¹⁰³Rh-¹H{³¹P} NMR: (19.12 MHz, C₇D₈) δ: -8738 (s).

Synthesis of compound [Ir₂(μ-Cl)₂P{[η²-(H-SiMe₂)CH₂C₆H₄][(o-C₆H₄)CH₂SiMe₂]}₂], 2Ir

In a Schlenk flask, compound **1** (71 mg, 0.15 mmol) and [IrCl(COD)]₂ (50 mg, 0.07 mmol) were degassed and then dissolved in pentane (1.5 mL). The solution was stirred for two hours at room temperature after which it was concentrated and kept overnight at 236 K. The resulting yellow solid was washed twice with 0.5 mL of cold pentane to yield a light yellow solid. Yield 97% (103 mg). IR (KBr): ν(Ir...H-Si) 2019 cm⁻¹, ω(Si-H) 796 cm⁻¹. ¹H NMR (400 MHz, C₆D₆, 293 K) δ: 6.99 (tt, ⁴J_{P-H} 1.6 Hz, ⁴J_{H-H} 1.6 Hz; ³J_{H-H} 7.6 Hz, 6H, CH_{aromatic}), 6.93 (dd, ³J_{P-H} 11.2 Hz; ³J_{H-H} 7.6 Hz, 6H, CH_{aromatic}), 6.86 (pt, ³J_{H-H} 5.6 Hz, 6H, CH_{aromatic}), 6.73 (dt, ⁴J_{P-H} 1.6 Hz, ³J_{H-H} 7.6 Hz, 6H, CH_{aromatic}), 2.13 (d, ²J_{H-H} 14.4 Hz, 6H, CH₂), 2.05 (dd, ²J_{H-H} 14.4 Hz; ⁴J_{P-H} 3.2 Hz, 6H, CH₂), 0.55 (br. s, ¹J_{Si-H} 42.0 Hz, 2H, σ(SiH)), 0.41 (s, 18H, CH₃), 0.53 (s, 18H, CH₃). ¹³C{¹H} NMR (C₆D₆, 175 MHz, 293 K) δ: 147.3 (d, ¹J_{P-C} 13.5 Hz, *C*_{ipso}-P), 132.5 (d, ²J_{P-C} 5.6 Hz, *C*_{ipso}-C), 131.6 (d, ³J_{P-C} 1.75 Hz, CH_{aromatic}), 131.5 (d, ²J_{P-C} 8.93 Hz, CH_{aromatic}), 128.6 (s, CH_{aromatic}), 125.3 (d, ³J_{P-C} 8.75 Hz, CH_{aromatic}), 27.6 (d, ³J_{P-C} 11.4 Hz, CH₂), 2.22 (s, CH₃), 2.93 (s, CH₃). ³¹P{¹H} NMR (161.9 MHz, C₆D₆, 293 K) δ: 0.21 (s).

Synthesis of [Rh₂(μ-Cl)₂P{(o-C₆H₄)CH₂SiMe₂}]₂O, 3Rh

Reaction of **2Rh** with adventitious water present in a toluene/Et₂O mixture led to the formation of yellow crystals which were filtrated and subsequently dried under vacuum. They were soluble in most laboratory solvents. Anal. Calcd for C₅₄H₇₂Cl₂O₂P₂Rh₂Si₆: C, 52.14; H, 5.79. Found: C, 51.56; H, 5.39. ¹H NMR (400 MHz, C₆D₆, 293 K) δ: 7.59 ppm (dd, ³J_{H-H} 7.2 Hz, ³J_{H-P} 4.9 Hz, 1H, CH), 7.14–6.94 (m, 5H, CH), 6.94–6.87 (m, 1H, CH), 6.77 (t, ³J_{H-H} 7.4 Hz, 1H, CH), 6.72–6.60 (m, 4H, CH), 3.63 (d, ²J_{H-H} 14.2 Hz, 1H, CH₂), 3.36 (d, ²J_{H-H} 13.9 Hz, 1H, CH₂), 2.89 (dd, ²J_{H-H} 14.5, ⁴J_{H-P} 3.0 Hz, 1H, CH₂), 2.33 (dd, ²J_{H-H} 14.1, ⁴J_{H-P} 7.3 Hz, 1H, CH₂), 2.01 (d, ²J_{H-H} 13.8 Hz, 1H, CH₂), 1.91 (ddd, ²J_{H-H} 14.2, ⁴J_{H-P} 7.1, ⁵J_{H-Rh} 2.0 Hz, 1H, CH₂), 1.28 (s, 3H, CH₃), 0.65 (s, 3H, CH₃), 0.59 (s, 3H, CH₃), 0.49 (s, 3H, CH₃), 0.05 (s, 3H, CH₃), -0.22 (s, 3H, CH₃). ¹³C{¹H} NMR (176.048 MHz, C₆D₆, 293 K) δ: 150.1 (d, ¹J_{C-P} 14.3 Hz, *C*_{ipso}-C), 148.2 (d, ²J_{C-P} 13.6 Hz, *C*_{ipso}-C), 144.1 (d, ²J_{C-P} 12.0 Hz, *C*_{ipso}-C η²-SiH), 133.8 (dd, *J*_{C-P} 16.3 Hz, *J*_{C-Rh} 4.4 Hz, CH_{aromatic}, 4C), 132.7 (d, *J*_{C-P} 6.8 Hz, CH_{aromatic}, 2C), 131.7 (d, *J*_{C-P} 8.1 Hz, CH_{aromatic}, 2C), 131.3 (s, *C*_{ipso}-C, 2C), 131.1 (t, *J*_{C-P} 7.7 Hz, CH_{aromatic}, 4C), 130.9 (s, *C*_{ipso}-C, 2C), 130.1 (s, *C*_{ipso}-C, 2C), 125.6 (d, *J*_{C-P} 8 Hz, CH_{aromatic}, 2C), 125.4 (dd, *J*_{C-P} 8.5, *J*_{C-Rh} 4.9 Hz, CH_{aromatic}, 4C), 33.3 (d, ³J_{C-P} 13.0 Hz, CH₂), 32.1 (d, ³J_{C-P} 8.0 Hz, CH₂), 28.7 (d, ³J_{C-P} 13.0 Hz, CH₂), 9.55 (s, CH₃), 5.20 (s, CH₃), 4.70 (s, CH₃), 3.81 (s, CH₃), 3.10 (s, CH₃), 2.95 (s, CH₃). ³¹P{¹H} NMR (161.9 MHz, C₆D₆, 293 K) δ: 26.20 (d, ¹J_{P-Rh} 157.1 Hz). ²⁹Si{³¹P} DEPT NMR (79.49 MHz, C₆D₆, 293 K) δ: 67.04 (s), 42.32 (s) and 5.37 (s). ¹⁰³Rh-¹H{³¹P} HMBC NMR (12.59 MHz, C₆D₆, 293 K) δ: -8416.73 ppm (s).

Synthesis of compound [Ir₂(μ-Cl)₂P{(o-C₆H₄)CH₂SiMe₂}]₂O, 3Ir

Reaction of compound 2Ir with adventitious water present in the working solvents, led to the formation of red-orange complex 3Ir featuring a siloxane bridge as in the case of the rhodium analogue. ¹H NMR (400 MHz, C₆D₆, 293 K) δ: 7.03–6.60 (m, 24H, CH_{aromatic}), 3.52, (d, ¹J_{H-H} 16 Hz, 2H, CH₂), 2.86 (dd, ¹J_{H-H} 16 Hz, ⁴J_{PH} 4 Hz, 2H, CH₂), 2.38 (dd, ¹J_{H-H} 12 Hz, ⁴J_{P-H} 4 Hz, 2H, CH₂), 2.18 (d, ¹J_{H-H} 12 Hz, 2H, CH₂), 2.17 (d, ¹J_{H-H} 12 Hz, 2H, CH₂), 2.03 (dd, ¹J_{H-H} 16 Hz, ⁴J_{P-H} 4 Hz, 2H, CH₂), 0.50 (s, 6H, CH₃), 0.45 (s, 6H, CH₃), 0.43 (s, 6H, CH₃), 0.36 (s, 6H, CH₃), 0.10 (s, 6H, CH₃) and -0.24 (s, 6H, CH₃). ³¹P{¹H} NMR (161.9 MHz, C₆D₆) δ -6.3 (s). ¹³C{¹H} NMR (176.008 MHz, C₇D₈, 293 K) δ: 32.6 (CH₂), 30.7 (CH₂), 26.5 (CH₂), 0.50 (CH₃), 0.49 (CH₃), 0.48 (CH₃), 1.13 (CH₃), 0.15 (CH₃), -0.18 (s, CH₃), all the aromatic carbons are in the range 120–150. ¹³C{¹H} NMR (176.008 MHz, C₆D₆, 293 K) δ 149.7 (d, ¹J_{P-C} 13 Hz, C_{ipso}-P), 148.1 (d, ¹J_{P-C} 12.4 Hz, C_{ipso}-P), 143.0 (d, ¹J_{P-C} 11 Hz, C_{ipso}-P), 133.2 (d, ³J_{P-C} 6 Hz, C_{ipso}-C), 133.0 (d, ³J_{P-C} 5.7 Hz, C_{ipso}-C), 132.9 (s, CH_{aromatic}), 132.5 (s, CH_{aromatic}), 132.1 (d, ³J_{P-C} 7.7 Hz, CH_{aromatic}), 131.4 (d, ³J_{P-C} 8.6 Hz, CH_{aromatic}), 131.2 (d, ³J_{P-C} 8.8 Hz, CH_{aromatic}), 130.8 (s, CH_{aromatic}), 130.7 (s, CH_{aromatic}), 130.5 (s, CH_{aromatic}), 129.8 (s, CH_{aromatic}), 128.0 (d, overlapped with the solvent signal, C_{ipso}-C), 125.1 (d, ²J_{P-C} 9 Hz, CH_{aromatic}), 124.9 (d, ²J_{P-C} 9.3 Hz, CH_{aromatic}), 124.8 (d, ²J_{P-C} 9.5 Hz, CH_{aromatic}), 32.6 (d, ³J_{P-C} 7.2 Hz, CH₂), 30.7 (d, ³J_{P-C} 9.8 Hz, CH₂), 26.4 (d, ³J_{P-C} 10.9 Hz, CH₂), 5.89 (s, CH₃), 3.39 (s, CH₃), 2.88 (s, CH₃), 2.71 (s, CH₃), 2.48 (s, CH₃), -0.05 (s, CH₃). ²⁹Si-¹H HMBC NMR (79.49 MHz, C₇D₈, 293 K) δ: 24.1 (br), 5.1 (br) and 3.5 (br).

Synthesis of [Rh₂(μ-Cl)₂P{(o-C₆H₄)CH₂SiMe₂Ph}]₂, 4Rh

To a Schlenk flask containing [RhCl(COD)]₂ (40 mg, 0.08 mmol) dissolved in 1 mL of benzene, [PhP{(o-C₆H₄)CH₂SiMe₂H}]₂ (65 mg, 0.16 mmol) was added under stirring and immediate evolution of gas was observed. Stirring was stopped after ca. 5 min and the reaction mixture was left to stand at room temperature. The resulting yellow crystals were filtered and washed twice with toluene. Yield 54% (47 mg). Anal. Calcd for C₄₈H₅₈Cl₂P₂Rh₂Si₄·C₆H₆: C, 55.72; H, 5.54. Found: C, 55.89; H, 5.34. The solubility of 4Rh was not enough for solution NMR studies and it reacted with CD₂Cl₂, CDCl₃ and DMSO-d₆. ¹H NMR (CP MAS) δ: 0.2 (CH₃), 2.2 (CH₂) and 7.1 (CH_{aromatic}). ¹³C (CP MAS) δ: 3.1 (CH₃), 6.0 (CH₃), 12.3 (CH₃), 28.7 (CH₂), 31.4 (CH₂), and for the aromatic carbons 123.3, 129.3, 131.9, 137.7, 147.1. ³¹P (CP MAS) δ: 45.3 (s). ²⁹Si (CP MAS) δ: 54.9 (s), 65.0 (s).

Synthesis of compound 4Ir

[IrCl(COD)]₂ (92.0 mg, 0.226 mmol) was added to a solution of [PhP{(o-C₆H₄)CH₂SiMe₂H}]₂ (76.1 mg, 0.113 mmol) in 0.6 mL of THF. Immediate evolution of gas was observed with concomitant formation of a yellow crystalline solid. After filtration, the solid was washed twice with cold THF (0.3 mL). Yield 72% (102.8 mg). Anal. Calcd for C₄₈H₅₈Cl₂P₂Ir₂Si₄: C, 45.58; H, 4.62.

Found: C, 45.42; H, 4.14. ¹³C (CP MAS) δ: 2.0, 2.8, 3.6, 8.9 (CH₃), 25.4, 28.6 (CH₂), from 122.6 to 147.5 (C_{aromatic}). ³¹P (P MAS) δ: 11.8 (br). ²⁹Si (CP MAS) δ: 22.7 (br), 13.8 (br).

Synthesis of [Rh{P{(o-C₆H₄)CH₂SiMe}Ph₂}₂Cl], 5Rh

To a 0.5 mL toluene solution of [RhCl(COD)]₂ (36 mg, 0.07 mmol), [Ph₂P{(o-C₆H₄)CH₂SiMe₂H}] (97 mg, 0.29 mmol) was added under stirring. The solution was left stirring overnight and then concentrated and stored at 273 K for 10 days. The yellow precipitate was washed twice with 0.5 mL of cold toluene. An off-brown solid was obtained. Yield 78% (44 mg). Anal. Calcd for C₄₂H₄₄ClP₂RhSi₂: C, 62.64; H, 5.51. Found: C, 62.03; H, 5.22. ¹H NMR (500 MHz, C₆D₆, 293 K) δ: 8.43 (s, 2H, CH), 8.07 (ψq, 2H, CH), 7.29 (m, 1H, CH), 7.13–6.91 (m, 2H, CH), 7.07–6.89 (m, 5H, CH_{aromatic}), 6.95–6.89 (m, 2H, CH), 2.08 (d, ²J_{H-H} 13.7 Hz, 1H, CH₂), 1.98 (vdt, ²J_{H-H} 13.8 Hz, ⁴J_{H-P} + ⁶J_{H-P} = 4.2 Hz, 1H, CH₂), 0.53 (s, 3H, CH₃), -0.42 (s, 3H, CH₃). ¹³C{¹H} NMR (100.61 MHz, C₆H₆, 293 K) δ: 148.3 (vt, ²J_{H-P} + ⁴J_{H-P} = 7.3 Hz, CH), 137.6 (vt, ³J_{H-P} + ⁵J_{H-P} = 7.3 Hz, CH_{aromatic}), 135.3 (br. s, CH), 133.1 (vt, ¹J_{H-P} + ²J_{H-P} = 23.3 Hz, CH_{aromatic}), 132.1 (vt, ²J_{H-P} + ⁴J_{H-P} = 3.0 Hz, CH), 131.6 (vt, ³J_{H-P} + ⁵J_{H-P} = 3.2 Hz, CH), 130.6 (s, CH), 130.4 (d, ⁴J_{P-Rh} 4 Hz, CH), 128.6 (vt, ³J_{H-P} + ⁵J_{H-P} = 4.9 Hz, CH), 125.1 (vt, ²J_{H-P} + ⁴J_{H-P} = 3.7 Hz, CH), 34.5 (vt, ³J_{H-P} + ⁵J_{H-P} = 9.9 Hz, CH₂), 9.80 (s, CH₃), 6.25 (d, ²J_{P-Rh} 1.9 Hz).

Crystal structure determination of 1, 3Rh, 4Rh, 5Rh, and 3Ir

See Table 1 and other details in the ESI.† The structures have been deposited at the Cambridge Crystallographic Data Centre (CCDC 1533794, 1533878, 1533806–1533808).

Acknowledgements

This work was supported by CONACyT (project 242818, PhD grants for MVCG, CACC, JZM and postdoctoral fellowship to ERF), ANR-CONACyT (274001), CNRS and Université Paul Sabatier. We also acknowledge the French-Mexican International Laboratory (LIA-LCMMC) for support.

Notes and references

- 1 K. J. Szabó and O. F. Wendt, *Pincer and Pincer-Type Complexes: Applications in Organic Synthesis and Catalysis*, Wiley, Weinheim, Germany, 2014.
- 2 G. van Koten and D. Milstein, in *Topics in Organometallic Chemistry*, Springer, Heidelberg, Germany, 2013, vol. 40, pp. 1–356.
- 3 C. Tsay, N. P. Mankad and J. C. Peters, *J. Am. Chem. Soc.*, 2010, **132**, 13975–13977.
- 4 D. Morales-Morales and C. Jensen, *The Chemistry of Pincer Compounds*, Elsevier, Amsterdam, 2007.
- 5 L. S. H. Dixon, A. F. Hill, A. Sinha and J. S. Ward, *Organometallics*, 2014, **33**, 653–658.

- 6 J. Choi, A. H. R. MacArthur, M. Brookhart and A. S. Goldman, *Chem. Rev.*, 2011, **111**, 1761–1779.
- 7 J. C. DeMott, W. Gu, B. J. McCulloch, D. E. Herbert, M. D. Goshert, J. R. Walensky, J. Zhou and O. V. Ozerov, *Organometallics*, 2015, **34**, 3930–3933.
- 8 C. S. Slone, D. A. Weinberger and C. A. Mirkin, in *Prog. Inorg. Chem.*, John Wiley & Sons, Inc., 2007, pp. 233–350.
- 9 M. S. Balakrishna, P. Chandrasekaran and P. P. George, *Coord. Chem. Rev.*, 2003, **241**, 87–117.
- 10 J. Y. Corey, *Chem. Rev.*, 2011, **111**, 863–1071.
- 11 J. Y. Corey, *Chem. Rev.*, 2016, **116**, 11291–11435.
- 12 K. S. Cook, C. D. Incarvito, C. E. Webster, Y. Fan, M. B. Hall and J. F. Hartwig, *Angew. Chem., Int. Ed.*, 2004, **43**, 5474–5477.
- 13 Z. Xiong, X. Li, S. Zhang, Y. Shi and H. Sun, *Organometallics*, 2016, **35**, 357–363.
- 14 T. Komuro, T. Arai, K. Kikuchi and H. Tobita, *Organometallics*, 2015, **34**, 1211–1217.
- 15 S. J. Mitton and L. Turculet, *Chem. – Eur. J.*, 2012, **18**, 15258–15262.
- 16 J. Yang and T. D. Tilley, *Angew. Chem., Int. Ed.*, 2010, **49**, 10186–10188.
- 17 A. M. Tondreau, J. M. Darmon, B. M. Wile, S. K. Floyd, E. Lobkovsky and P. J. Chirik, *Organometallics*, 2009, **28**, 3928–3940.
- 18 L. Turculet, J. D. Feldman and T. D. Tilley, *Organometallics*, 2004, **23**, 2488–2502.
- 19 S. C. Bart, E. Lobkovsky and P. J. Chirik, *J. Am. Chem. Soc.*, 2004, **126**, 13794–13807.
- 20 P. B. Glaser and T. D. Tilley, *J. Am. Chem. Soc.*, 2003, **125**, 13640–13641.
- 21 X. Du and Z. Huang, *ACS Catal.*, 2017, **7**, 1227–1243.
- 22 D. Troegel and J. Stohrer, *Coord. Chem. Rev.*, 2011, **255**, 1440–1459.
- 23 P. Sangtrirutnugul and T. D. Tilley, *Organometallics*, 2007, **26**, 5557–5568.
- 24 M. C. Lipke, A. L. Liberman-Martin and T. D. Tilley, *Angew. Chem., Int. Ed.*, 2017, **56**, 2260–2294.
- 25 M. C. Lipke, A. L. Liberman-Martin and T. D. Tilley, *J. Am. Chem. Soc.*, 2016, **138**, 9704–9713.
- 26 H. Kameo, S. Ishii and H. Nakazawa, *Dalton Trans.*, 2012, **41**, 11386–11392.
- 27 S. Park and M. Brookhart, *Organometallics*, 2010, **29**, 6057–6064.
- 28 J. Yang and M. Brookhart, *J. Am. Chem. Soc.*, 2007, **129**, 12656–12657.
- 29 S. R. Klei, T. D. Tilley and R. G. Bergman, *Organometallics*, 2002, **21**, 4648–4661.
- 30 Y. Li, Y. Feng, L. Xu, L. Wang and X. Cui, *Org. Lett.*, 2016, **18**, 4924–4927.
- 31 R. M. Martin, R. G. Bergman and J. A. Ellman, *J. Org. Chem.*, 2012, **77**, 2501–2507.
- 32 K. Parthasarathy, M. Jeganmohan and C.-H. Cheng, *Org. Lett.*, 2008, **10**, 325–328.
- 33 J. Yang, P. S. White and M. Brookhart, *J. Am. Chem. Soc.*, 2008, **130**, 17509–17518.
- 34 J. L. McBee, J. Escalada and T. D. Tilley, *J. Am. Chem. Soc.*, 2009, **131**, 12703–12713.
- 35 G. Mancano, M. J. Page, M. Bhadbhade and B. A. Messerle, *Inorg. Chem.*, 2014, **53**, 10159–10170.
- 36 S. Gatard, C.-H. Chen, B. M. Foxman and O. V. Ozerov, *Organometallics*, 2008, **27**, 6257–6263.
- 37 E. Calimano and T. D. Tilley, *J. Am. Chem. Soc.*, 2008, **130**, 9226–9227.
- 38 S. B. Duckett, D. M. Haddleton, S. A. Jackson, R. N. Perutz, M. Poliakoff and R. K. Upmacis, *Organometallics*, 1988, **7**, 1526–1532.
- 39 M. J. Fernandez, P. M. Bailey, P. O. Bentz, J. S. Ricci, T. F. Koetzle and P. M. Maitlis, *J. Am. Chem. Soc.*, 1984, **106**, 5458–5463.
- 40 X. Zhou and S. R. Stobart, *Organometallics*, 2001, **20**, 1898–1900.
- 41 S. R. Stobart, X. Zhou, R. Cea-Olivares and A. Toscano, *Organometallics*, 2001, **20**, 4766–4768.
- 42 G. W. Bushnell, M. A. Casado and S. R. Stobart, *Organometallics*, 2001, **20**, 601–603.
- 43 R. D. Brost, G. C. Bruce, F. L. Joslin and S. R. Stobart, *Organometallics*, 1997, **16**, 5669–5680.
- 44 M. J. Auburn, R. D. Holmes-Smith, S. R. Stobart, P. K. Bakshi and T. S. Cameron, *Organometallics*, 1996, **15**, 3032–3036.
- 45 E. Sola, A. García-Camprubí, J. L. Andrés, M. Martín and P. Plou, *J. Am. Chem. Soc.*, 2010, **132**, 9111–9121.
- 46 V. Montiel-Palma, M. A. Muñoz-Hernández, C. A. Cuevas-Chávez, L. Vendier, M. Grellier and S. Sabo-Etienne, *Inorg. Chem.*, 2013, **52**, 9798–9806.
- 47 V. Montiel-Palma, M. A. Munoz-Hernandez, T. Ayed, J.-C. Barthelat, M. Grellier, L. Vendier and S. Sabo-Etienne, *Chem. Commun.*, 2007, 3963–3965.
- 48 C. A. Tolman, *Chem. Rev.*, 1977, **77**, 313–348.
- 49 V. Tedesco and W. von Philipsborn, *Magn. Reson. Chem.*, 1996, **34**, 373–376.
- 50 I. Lee, F. Dahan, A. Maisonnat and R. Poilblanc, *Organometallics*, 1994, **13**, 2743–2750.
- 51 F. Delpech, S. Sabo-Etienne, B. Donnadiu and B. Chaudret, *Organometallics*, 1998, **17**, 4926–4928.
- 52 M. Aizenberg, J. Ott, C. J. Elsevier and D. Milstein, *J. Organomet. Chem.*, 1998, **551**, 81–92.
- 53 T. Konno, K. Tokuda, J. Sakurai and K.-I. Okamoto, *Bull. Chem. Soc. Jpn.*, 2000, **73**, 2767–2773.
- 54 M. Okazaki, S. Ohshitanai, H. Tobita and H. Ogino, *J. Chem. Soc., Dalton Trans.*, 2002, 2061–2068.
- 55 S. G. Koller, R. Martín-Romo, J. S. Melero, V. P. Colquhoun, D. Schildbach, C. Strohmman and F. Villafañe, *Organometallics*, 2014, **33**, 7329–7332.
- 56 M. Okazaki, S. Ohshitanai, M. Iwata, H. Tobita and H. Ogino, *Coord. Chem. Rev.*, 2002, **226**, 167–178.
- 57 J. F. Riehl, Y. Jean, O. Eisenstein and M. Pelissier, *Organometallics*, 1992, **11**, 729–737.
- 58 E. E. Korshin, G. Leitius, L. J. W. Shimon, L. Konstantinovski and D. Milstein, *Inorg. Chem.*, 2008, **47**, 7177–7189.

- 59 J. D. Feldman, J. C. Peters and T. D. Tilley, *Organometallics*, 2002, **21**, 4065–4075.
- 60 T. Cuenca and P. Royo, *Coord. Chem. Rev.*, 1999, **193–195**, 447–498.
- 61 M. Barquín, M. A. Garralda, L. Ibarlucea, C. Mendicute-Fierro, E. Pinilla, V. San Nacianceno and M. R. Torres, *Organometallics*, 2011, **30**, 1577–1587.
- 62 D. Y. Wang, Y. Choliy, M. C. Haibach, J. F. Hartwig, K. Krogh-Jespersen and A. S. Goldman, *J. Am. Chem. Soc.*, 2016, **138**, 149–163.
- 63 G. Giordano and R. H. Crabtree, *Inorg. Synth.*, 1979, **19**, 218–220.
- 64 G. W. Parshall, *Inorg. Synth.*, 1974, **15**, 18.